

Excitonic processes in pure and doped CaF_2

This article has been downloaded from IOPscience. Please scroll down to see the full text article.

1999 J. Phys.: Condens. Matter 11 3115

(<http://iopscience.iop.org/0953-8984/11/15/016>)

View [the table of contents for this issue](#), or go to the [journal homepage](#) for more

Download details:

IP Address: 171.66.16.214

The article was downloaded on 15/05/2010 at 07:18

Please note that [terms and conditions apply](#).

Excitonic processes in pure and doped CaF₂

V Denks†, A Maaros†, V Nagirnyi†, T Savikhina† and V Vassiltsenko‡

† Institute of Physics, University of Tartu, Riia 142, EE2400 Tartu, Estonia

‡ Physics Department, University of Tartu, Tähe 4, EE2400 Tartu, Estonia

Received 17 December 1998

Abstract. The optical properties of nominally pure CaF₂ crystals as well as of those of pure and Li⁺-, Na⁺-, Mg²⁺- and Mn²⁺-doped CaF₂ powders are compared. The emission band peaking at 3.9 eV and the excitation bands in the region 10–10.6 eV observed for CaF₂:Li and CaF₂:Na powders are ascribed to the radiative decay of a self-trapped exciton perturbed by an anion vacancy or impurity–vacancy dipole. A Mn²⁺-perturbed exciton has been found in CaF₂:Mn.

1. Introduction

The phenomenon of the decay of elementary electronic excitations into a pair of Frenkel defects plays a crucial role in the radiation or laser damage (coloration, surface and volume damage) of optical materials (see, e.g., [1, 2]). The present paper represents a continuation of an investigation started in [3] of the influence of intrinsic and impurity defects on the excitonic processes in CaF₂, one of the two main optical materials for the spectral region $\lambda < 200$ nm [4, 5]. Another important optical material, MgF₂, is optically a uniaxial crystal, which hampers its application if the volume and time structure of the laser pulse are to be retained.

The situation concerning the optical materials for short-wavelength regions became more drastically bad with the discovery of a new type of laser damage of quartz glass: the change of density and, correspondingly, the refraction coefficient in the laser beam periphery region [6]. This kind of damage is likely to be connected with the amorphous glass structure, which initially possessed some spatial inhomogeneity. No similar damage effect is observed for crystalline materials. So, in spite of the continuous search for a new, possibly fluorine-containing, glass for the region $\lambda < 200$ nm (see, e.g., [7]), it is clear that it is impossible to solve all of the problems with the aid of a glass material. Therefore, we consider the investigation of the elementary processes of CaF₂ crystal damage, with a view to possible improvement of its radiation and laser stability, to be now of utmost importance.

We investigated the possibility of raising the volume resistance of CaF₂ crystal to laser or radiation damage by doping the material with some metal impurity. An impurity ion was thought to trap an exciton and to raise its probability of radiative decay, preventing, in a such way, the decay of the exciton into lattice defects. Different impurities were studied with two main purposes: (i) to estimate an optimal concentration of impurity ions as regards the free passage of excitons; and (ii) to investigate the mechanisms of energy transfer from the lattice to an impurity ion for different doping ions. For technological reasons, the preliminary study was more suitable for performing on a powdered material, with the results subsequently extended to crystals. In this investigation we have found an impurity which might significantly raise the radiation resistance of CaF₂; this is, however, the subject of our next publication. In the

present paper we would like to summarize the results obtained during this investigation that are important for the physics of electronic excitation in doped fluorite systems, and are applicable both to powdered and crystalline materials.

2. Materials and methods

The material for this investigation has been selected from among five available nominally pure CaF_2 crystals of different origins, obviously containing different amounts of unintentionally introduced impurities. The selection was based on the results of a study of transmission spectra for the energy region 3.5–10.5 eV, impurity luminescence spectra for the region 2–5 eV under VUV, x-ray or pulsed electron-beam excitation, and ionic conductivity in the temperature region 300–1200 K. The transmission and luminescence spectra were measured both for polished and for cleaved samples.

The purest selected material was ground to powder and doped with Mg^{2+} , Na^+ or Li^+ , using the thermodiffusion method. The mixtures of CaF_2 and LiF , NaF or MgF_2 powders were heated for 30 min in a platinum crucible, placed into a pumped and soldered quartz ampoule. The heating temperatures varied from 800 to 1100 °C for $\text{CaF}_2:\text{LiF}$ and $\text{CaF}_2:\text{NaF}$, and from 800 to 1200 °C for $\text{CaF}_2:\text{MgF}_2$. All of the impurity concentrations indicated in this paper are given in weight per cent in a powder mixture. All of the measured spectral and electrical characteristics of the doped powders were compared to those of the basic material, i.e. undoped powders that had undergone the same thermal treatment. A powdered $\text{CaF}_2:\text{Mn}$ phosphor, synthesized at the University of Tartu, was also investigated. In that case the initial undoped powder was used for the comparison.

A sample to be investigated was mounted in a vacuum nitrogen cryostat. A hydrogen discharge lamp and a vacuum monochromator were used for excitation in the regions 4–13.5 eV at room temperature and 4–12 eV at 85 K. The latter restriction was imposed by the LiF cryostat window. The emission of the samples investigated was selected by a grating monochromator or a system of optical filters. The luminescence under x-ray excitation (25 kV, 0.5 mA) was studied at 85 and 295 K. The decay kinetics was measured under pulsed-electron-beam excitation (2 ns, 300 keV, 100 A cm^{-2}). All necessary corrections were made to the measured emission and excitation spectra.

3. Experimental results

3.1. Transition from single crystal to powder

The emission and excitation spectra of the best selected single CaF_2 crystal, measured at 295 K, are shown in figure 1(a) (curves 1 and 1', respectively). Curve 4 represents the absorption spectrum at 295 K [8]. Arrows indicate the excitonic absorption maximum (E_e) and the edge of the interband transitions (E_g) [9]. The emission and excitation spectra of the best selected CaF_2 crystal (curves 2 and 2', respectively) and those of the powder produced from the same crystal (curves 3 and 3') measured at 85 K are compared in figure 1(b). The emission of self-trapped excitons dominates for all of our samples. The emission bands connected with unintentionally introduced impurities and lattice defects are weaker by two orders of magnitude. The position of the maximum of the excitonic band for the single crystal is the same as that reported in [10, 2] (4.44 eV at 77 K). For the powdered material, the edge of the excitation spectrum of the excitonic emission is shifted towards higher energies (compare curves 2' and 3'). A similar effect was observed in [11]. The efficiency of the main emission is high under the excitation in the excitonic absorption band and that in the region of interband

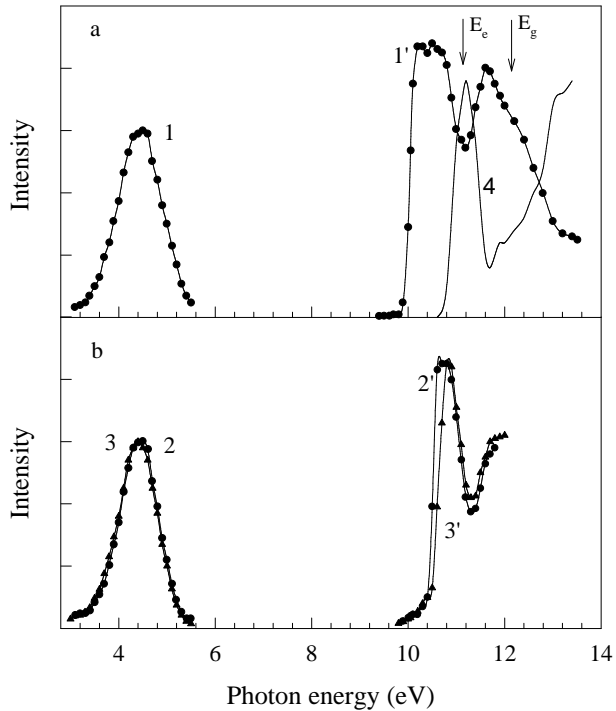


Figure 1. The emission (curves 1–3) and excitation (curves 1'–3') spectra of a single CaF₂ crystal (curves 1, 1', 2, 2') and of the powder produced from the same crystal (curves 3, 3'), measured at 295 K (a) and 85 K (b). Curve 4 represents the absorption spectrum at 295 K [8]. Arrows indicate the excitonic absorption maximum (E_e) and the edge of the interband transitions (E_g) [9].

transitions. At room temperature this emission is quenched by about 60%. The activation energy for quenching is $E_a \approx 0.42$ eV, which is in good agreement with the data of [11–13].

3.2. Systems with Mg²⁺ and Mn²⁺ impurity cations

Figure 2 shows the emission spectra of CaF₂ doped with $\approx 0.1\%$ of Mg²⁺ at 1200 °C (curve 2) and undoped CaF₂ heated at 1200 °C (curve 1), measured at 85 K, under excitation in the excitonic absorption peak ($E_{exc} = 11.2$ eV). Under the excitation at 10.1 eV a weak additional emission band appears at about 3.8 eV for both powders (curves 4 and 3, respectively). This emission is absent for unheated pure powder, its intensity rises with the rise of the heating temperature, and it can obviously be excited only near the fundamental absorption edge at 9.9–10.3 eV. We could not investigate this emission in more detail due to its low intensity. According to our data, the introduction of Mg²⁺ in CaF₂ causes only a small shift of the low-energy edge of the excitation spectrum (compare curves 1' and 2', measured for pure and doped CaF₂, respectively), a slight rise in ionic conductivity, and a doubling of the intensity of the weak 3.8 eV emission.

The main conclusion drawn from this investigation is as follows. Upon introduction of Mg²⁺ in CaF₂ to a concentration of 0.01–0.1%, no defects are created in the material that are capable of trapping elementary electronic excitations with appreciable efficiency at temperatures higher than 85 K. This means that substitution of isovalent Mg²⁺ ions (ion radius $r = 0.86$ Å) for Ca²⁺ ($r = 1.14$ Å) at cation sites in CaF₂ does not cause any significant

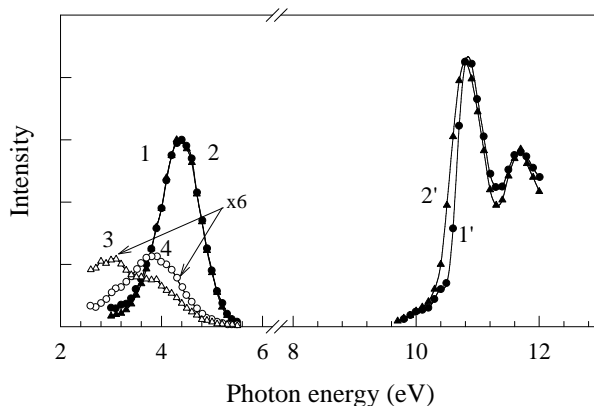


Figure 2. The emission (curves 1–4) and excitation (curves 1' and 2') spectra of CaF₂ powder doped with $\approx 0.1\%$ of Mg²⁺ at 1200 °C (curves 2, 2', 4) and of an undoped CaF₂ powder heated to 1200 °C (curves 1, 1', 3), measured at 85 K under excitation at 11.2 eV (curves 1, 2) and 10.1 eV (curves 3, 4).

distortions of the surrounding lattice which might influence the excitonic processes with appreciable efficiency.

Another system with a bivalent impurity, CaF₂:Mn, is of special interest because of the high luminescence efficiency of this luminophor, and in view of its application in thermoluminescent dosimetry (see, e.g., [14, 15]). The emission and excitation spectra of CaF₂:Mn (0.2%) at 295 and 85 K are shown in figures 3(a) and 3(b). The emission band at 2.5 eV, connected with Mn²⁺ centres [16], is a dominant one in the emission spectra (curves 1). Its efficiency is high under excitation in the region of the absorption bands at 8, 8.7, and 9.8 eV (see [17] for the Mn²⁺ absorption bands at energies lower than 7.2 eV) as well as in the excitonic region (10.5–11.8 eV) and in the region of interband transitions ($E_{exc} > 11.8$ eV) (curves 1'). This indicates a high efficiency of the energy transfer from a crystal matrix to an impurity centre in this system. Due to this, the excitonic emission at 4.4 eV is strongly suppressed even under excitation in the maximum of the excitonic absorption band (curves 1). The excitation spectrum of the emission of self-trapped excitons at 295 K, measured for the same undoped CaF₂ material, is shown in figure 3(a), curve 2'.

A new emission band appears for Mn²⁺-doped CaF₂, which is of special interest for this investigation. It is situated at lower energies than the excitonic emission, peaking at about 4 eV (figure 3(b), curve 3). This emission is excited mainly at the low-energy edge of the fundamental absorption of CaF₂, whereas a distinct maximum at 10.4 eV is observed in the excitation spectrum at 85 K (curve 3'). At higher energies the excitation spectrum is distorted due to a strong overlapping of the 4 eV band with the emission band of the self-trapped excitons. No explicit anomaly at 10.4 eV can be observed in the excitation spectrum at 295 K due to a long-wavelength shift of the fundamental absorption.

Thus, in contrast to the case for Mg²⁺ impurity, the introduction of a Mn²⁺ ion ($r = 0.91$ Å) into the calcium sites of a fluorite leads to the appearance of a new luminescence centre absorbing light at 10.4 eV and emitting it at 4 eV. One may conclude that the distortion of the lattice around an impurity Mn²⁺ ion is sufficiently strong to cause a displacement of the surrounding F⁻ ions towards an impurity, and a corresponding split of a local energy level from an excitonic zone. Electronic transitions to this level are obviously responsible for the excitation band at 10.4 eV. After the relaxation of this electronic excitation, an impurity-trapped

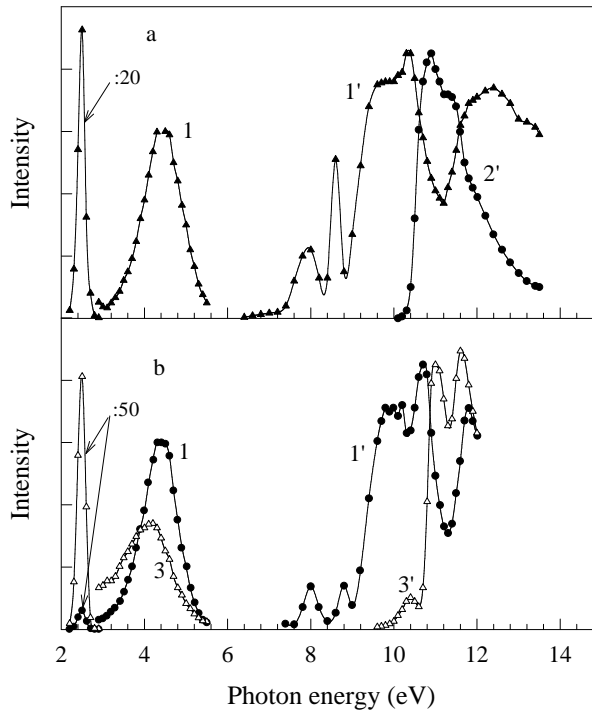


Figure 3. The emission spectra of a CaF₂:Mn (0.2%) powder (curves 1, 3) at 295 K (a) and 85 K (b) under excitation at 11.2 eV (curve 1) and 10.1 eV (curve 3) and the excitation spectra of the 2.5 eV (curve 1') and 3.9 eV emission (curve 3') of a CaF₂:Mn (0.2%), and the 4.4 eV emission of an undoped CaF₂ powder (curve 2').

exciton is created, whereas its emission band is likely to shift (by ≈ 0.4 eV) to the low-energy side with respect to the emission of a self-trapped exciton.

The coincidence of the maximum at 10.4 eV in the excitation spectrum of an impurity-trapped exciton (figure 3(b), curve 3') with the gap observed at the same energy in the excitation spectrum of the impurity emission (curve 1') may imply the absence of a resonance energy transfer from this exciton to a Mn²⁺ ion. In contrast to our results for CaF₂:Mn, a resonant energy transfer to impurity centres has been established for CaF₂:Eu in [18]. The situation is different for CaF₂:Pb [19], where under excitation at 9.6 eV in the D absorption band connected with an exciton localized near Pb²⁺, the relaxation also occurs into the A state of the Pb²⁺ centre. It is worth mentioning that the magnitude of the CaF₂ lattice distortion by a Pb²⁺ ion ($r = 1.33$ Å) is much larger than that in the case of a Mn²⁺ ion and, correspondingly, the absorption band of impurity-perturbed F⁻ in CaF₂:Pb (9.6 eV) is shifted much more with respect to the CaF₂ excitonic peak than in CaF₂:Mn (10.4 eV).

3.3. Systems with Na⁺ and Li⁺ cation impurities

Upon the introduction of the monovalent alkaline metals Li, Na, K, Rb at the cation sites of fluorites, the compensation of extra negative charge is accomplished due to the generation of anion (fluorine) vacancies v_a^+ (see, e.g., [1, 20–22]). Following the terminology of alkali halide physics, let us refer to an anion vacancy as an α -centre. Three main defect groups are created in a crystal doped by the methods described in section 2: single α -centres with concentration

N_α , single impurity cations M_S^+ with the same concentration, and impurity–vacancy dipoles $M_S^+-\alpha$ with concentration N_D . The binding energy is 0.76 eV for a $Na^+-\alpha$ dipole [20] and about 0.2 eV less for a $Li^+-\alpha$ dipole [22]. This means that a considerable fraction of the dipoles are dissociated at room temperature.

Single and dipole defects have been studied in detail for $CaF_2:Ln$ systems, where Ln denotes all lanthanides, as well as for $CaF_2:Y$ (see, e.g., [1, 23] and references therein). These defects are Ln^{3+} at calcium sites, interstitial F_i^- ions non-locally compensating for Ln^{3+} extra charge, and $Ln^{3+}-F_i$ dipoles. The dipole binding energies in such systems lie in the region 0.4–0.7 eV, and at impurity concentrations below 0.1 mol% the concentrations of single defects and dipoles are almost equal in order of magnitude. This leads us to the suggestion that for $CaF_2:Na$ and $CaF_2:Li$, having similar dipole binding energies, the N_α - and N_D -values are comparable, although the ratio N_α/N_D might be different for Na- and Li-doped CaF_2 .

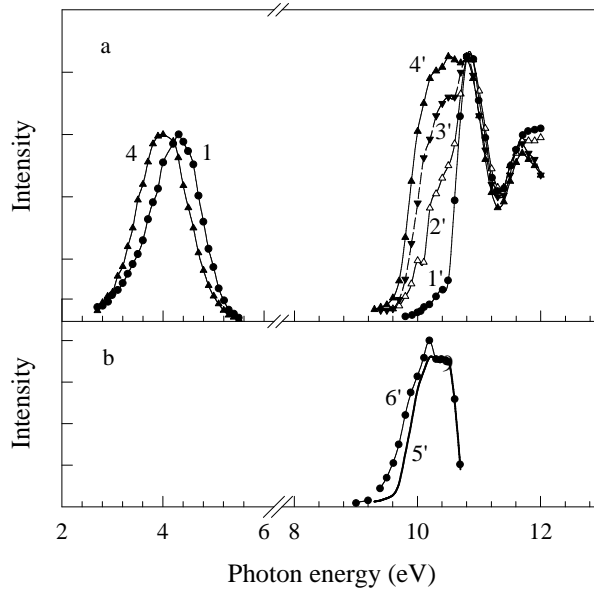


Figure 4. The emission spectra (curves 1, 4) and the excitation spectra of the total emission (curves 1'–4', 6') of an undoped CaF_2 powder (curves 1, 1') and $CaF_2:Na$ powders with Na concentrations of 0.01% (curve 2'), 0.03% (curve 3'), and 0.1% (curves 4, 4') at 85 K. Curves 1 and 4 were measured under excitation at 11.2 and 10.3 eV, respectively. Curve 5' represents the difference between curves 4' and 1'. Curve 6' represents the excitation spectrum for 3.8 eV emission.

This suggestion would provide an unambiguous explanation of the spectral characteristics measured at 85 K for different concentration sequences of the $CaF_2:Na$ (figure 4) and $CaF_2:Li$ (figure 5) systems. As the impurity concentration rises in both systems (figure 4(a), curves 1'–4' and figure 5(a), curves 1'–3'), or the doping temperature grows (figure 5(b), curves 1', 5', 6'), two new excitation bands appear and grow below the edge of the CaF_2 fundamental absorption in the excitation spectrum measured for an integrated ultraviolet emission through an ultraviolet optical filter. The appearance of the two new excitation bands may be seen more clearly in differential spectra (figure 4(b), curve 5' and figure 5, curves 4', 7'). A new emission band peaking at 3.9 eV is efficiently excited in the region of 9.4–10.7 eV (figure 4(a), curve 4 and figure 5(a), curve 3). Two excitation bands near 10 eV are also clearly seen in the excitation spectrum of the 3.9 eV emission selected by a monochromator (figure 4(b), curve 6'). The

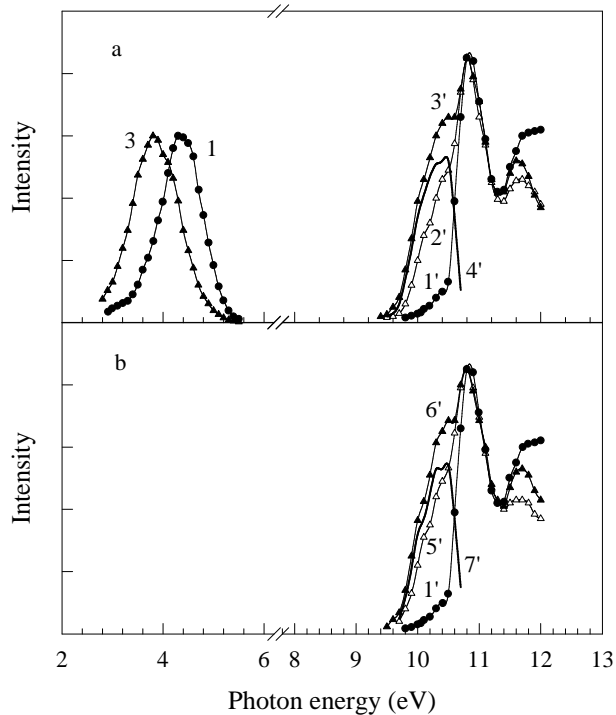


Figure 5. The emission spectra (curves 1, 3) and the excitation spectra of the total emission (curves 1'–3', 5', 6') of an undoped CaF₂ powder (curves 1, 1'), and of CaF₂:Li powders with Li concentrations of 0.003% (curve 2') and 0.03% (curves 3, 3'), and of CaF₂:Li (0.03%) doped at 800 (curve 5') and 900 °C (curve 6'), measured at 85 K. Curves 1 and 3 were measured under excitation at 11.2 and 10.3 eV, respectively. Curves 4' and 7' represent the results of subtraction of curve 1' from curves 3' and 6', respectively.

maxima of these bands are situated at ≈ 10.2 and ≈ 10.6 eV in both systems and their position seems to be independent of which monovalent impurity cation is present.

On the basis of the wealth of experience in alkali halide crystal physics, the following model may be suggested for the interpretation of the observed excitation bands. The excitation band at ≈ 10.2 eV is an α -band, connected with electronic transitions in F⁻ ions surrounding a single anion vacancy (an α -centre). The ≈ 10.6 eV band originates from the absorption by F⁻ ions situated near M_S⁺- α dipoles. Finally, the absorption by F⁻ ions surrounding a single M_S⁺ ion is expected to be shifted towards higher energies with respect to the excitonic peak and cannot be observed due to the overlap with the fundamental absorption. Correspondingly, the luminescence at 3.9 eV may be ascribed to the radiative decay of a relaxed exciton perturbed by a α -centre (α -luminescence).

The ionic conductivity (σ) of undoped CaF₂ at $T \approx 400$ – 900 K is caused by mobile α -centres with activation energies ≈ 0.55 eV [1, 20]. This is the so-called intrinsic defect conductivity. As the concentration of impurity M_S⁺ cations is increased, the number of single α -centres also increases and causes a rise of σ in the same temperature region. The same effect is observed in all of our systems and is observable in figure 6, showing the dependence of $\log(\sigma T)$ on $1/T$ for some of our samples.

We compared the concentration dependence of the amount by which the α -luminescence intensity at 10.1 eV excitation of the doped powder exceeds that for an undoped sample

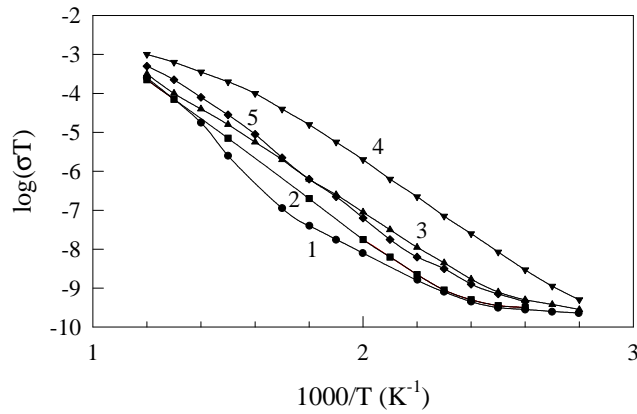


Figure 6. The dependence of $\log(\sigma T)$ on the inverse temperature for undoped CaF_2 (curve 1), $\text{CaF}_2:\text{Mg}$ (0.1%) (curve 2), $\text{CaF}_2:\text{Na}$ (0.03%) (curve 3), $\text{CaF}_2:\text{Na}$ (0.1%) (curve 4), and $\text{CaF}_2:\text{Li}$ (0.1%) (curve 5). σ is the ionic conductivity.

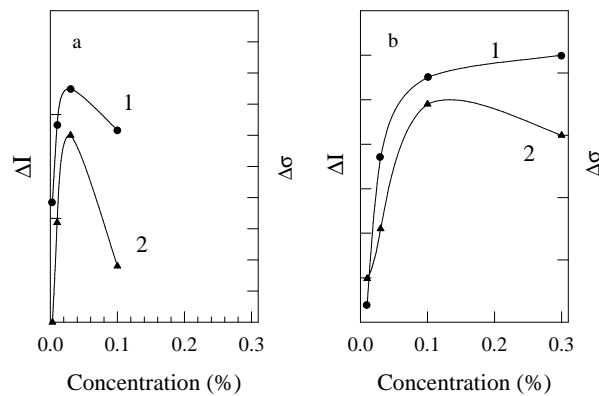


Figure 7. The dependence of the increase of the luminescence intensity ΔI (curve 1) and the differential increase of the ionic conductivity $\Delta\sigma$ at 500 K (curve 2) on the impurity concentration in $\text{CaF}_2:\text{Li}$ (a) and $\text{CaF}_2:\text{Na}$ (b).

(ΔI) with the concentration dependence of the differential increase of conductivity $\Delta\sigma$ at $T = 500$ K (figure 7). A sufficiently good correlation is observed for both systems, giving a direct confirmation of our model. Also, it should be mentioned that the increase of ΔI and $\Delta\sigma$ terminates in $\text{CaF}_2:\text{Li}$ at lower concentrations than in $\text{CaF}_2:\text{Na}$. This circumstance is in agreement with the higher isomorphous solubility of sodium in a fluorite lattice (see, e.g., [1]).

Transmission spectra for a sequence of concentrations of Na^+ in $\text{CaF}_2:\text{Na}$ crystals were measured in [21]. The α -band was not discovered, but the conclusion was drawn that its maximum is to be expected at $E > 9.9$ eV which is in agreement with the value obtained for our samples.

Excitons localized near an α -centre (with the excitation band at ≈ 10.2 eV) and those localized near an $\text{M}_S^+-\alpha$ dipole (with the excitation band at ≈ 10.6 eV) are situated at crystal sites with different degrees of deformation. This circumstance will inevitably lead to differences in some luminescence characteristics of the two excitons. We could not find any spectral differences in the broad 3.9 eV emissions under excitation at 10.2 and 10.6 eV. However,

we established that there were two stages in the thermal quenching of the 3.9 eV emission. The first, low-temperature one has the activation energies $E_{a1} \approx 0.07$ eV for CaF₂:Li and $E_{a1} \approx 0.09$ eV for CaF₂:Na. During this stage, the intensity decreases by about a third from the initial value. The activation energy for the second stage is $E_{a2} \approx 0.25$ eV and this coincides within the experimental error range for CaF₂:Li and CaF₂:Na. Within the framework of our model of trapped excitons in CaF₂:Na and CaF₂:Li, the first quenching stage may be connected with the excitons localized at the dipoles, whereas the second one may be connected with the excitons localized at α -centres. The excitation spectra of the 3.9 eV emission, measured after the end of the first stage at $T > 160$ K, show no anomalies at 10.6 eV. The connection of the 10.2 and 10.6 eV excitation peaks with α -centres and dipoles is confirmed also by our investigation of x-irradiated samples. That is, the intensities of these peaks decrease for x-irradiated CaF₂:Na (0.01%) more strongly than that of the excitonic peak at 11.3 eV. This intensity decrease may be connected with the decrease of the number of anion vacancies due to an efficient trapping of electrons. As a result, F centres are created in an x-irradiated sample.

Thermal bleaching and thermally stimulated luminescence (TSL) of CaF₂ crystals irradiated by fast neutrons at 20 K have been investigated in [24]. It has been shown that an intense 3.87 eV band is observed in the TSL spectrum at 130 K, when thermally released V_K centres recombine with F centres. As a result of such recombination, an exciton of the $V_K e^-$ type is obviously created in the vicinity of an anion vacancy. This exciton has the same luminescence properties as those of α -luminescence, studied in present paper.

Theoretical consideration has been given in [25] to the effect of an anion vacancy in CaF₂ on the energy levels of the surrounding ions. It has been shown that such a defect should cause the splitting of the local level from the bottom of the conduction band and a lowering of its energy to 4 eV. Our experiment gives the shift value of ≈ 1 eV (11.2–10.2 eV) for both CaF₂:Na and CaF₂:Li.

One of the main characteristics of a luminescence centre, an exciton in our case, is its decay time τ . The decay curves for CaF₂, CaF₂:Na (0.1%) and CaF₂:Li (0.03%) were measured under pulsed electron-beam excitation at 85 K. Only one weak (a few per cent in the total light sum) fast component with $\tau_1 \approx 12$ ns was registered in the decay kinetics of the excitonic emission at 4.4 eV for a pure material. The decay time of the slow component ($\tau_2 > 100$ ns) was beyond the operation time of our set-up. These results agree with the published data: $\tau_1 \approx 10$ – 20 ns, $\tau_2 \approx 40$ – 50 μ s; the intensity of the fast component constitutes a few per cent of the total light sum [10, 12, 13, 26]. In the case of doped materials, the α -band at 3.9 eV is dominant in the emission spectrum under electron-beam excitation. The fast component with $\tau_1 \approx 12$ ns is the most intense one for CaF₂:Na while the component with $\tau_1 \approx 7$ ns dominates in the case of CaF₂:Li. The slow component with $\tau_2 > 100$ ns was also registered for both systems; its intensity, however, amounted to only a few per cent of the total intensity.

It is possible to conclude from the latest results that, under electron-beam excitation, when self-trapped excitons and impurity-trapped excitons are created, mainly upon electron-hole recombination, the emission balance is significantly shifted towards the defect-perturbed excitons.

4. Conclusions

The main process of the dissipation of the energy absorbed by a material with self-trapped excitons is the annihilation of self-trapped and impurity-trapped excitons. This process may occur in three competing ways. These are via a luminescent channel, a non-radiative multiphonon (thermal) channel, and a non-radiative channel with defect creation. The investigation of these three channels would we hope result in an exposition of the methods of

the enhancement of the role of the two first channels and, subsequently, in improvements in the radiation and laser stabilities of materials.

In the present paper we discovered and investigated a sequence of excitons perturbed by different intrinsic and impurity defects in CaF₂ optical material. The main parameters of these excitons at 85 K are summarized in table 1. The decay time of the intense fast component of an impurity-perturbed exciton is 12 ns for CaF₂:Na and 7 ns for CaF₂:Li at 85 K. We did not find any manifestations of an exciton localized near the Mg²⁺ ion in CaF₂. None of the impurities described in the present paper led to an improvement of the radiation stability of CaF₂. However, the results of this investigation give an important key to the comprehension of exciton relaxation in doped crystals. It is clear that in CaF₂, doped with monovalent impurities, the exciton is trapped due to a lattice distortion around the doping-induced anion vacancy. The so-called α -emission is connected with excitons of this type. In the case of bivalent cation impurities of small radius, such as are present in CaF₂:Mg, there might be no exciton trapping.

Table 1. Parameters for perturbed excitons in doped CaF₂ ($h\nu_m^x$: absorption band maximum; ΔE : distance from the intrinsic excitonic peak at 11.2 eV; $h\nu_m^e$: emission band maximum).

Defect	$h\nu_m^x$ (eV)	ΔE (eV)	$h\nu_m^e$ (eV)
α -centre (v_a^+)	10.2	1.0	3.9
Na ⁺ - v_a^+ dipole	10.6	0.6	3.9
Li ⁺ - v_a^+ dipole	10.6	0.6	3.9
Mn ²⁺	10.4	0.8	4.0
Pb ²⁺ [16]	9.6	1.6	—

In the case of non-isovalent cation impurities (Na⁺, Li⁺ and so on), centres that efficiently trap electronic excitations are created in CaF₂ (α -centres, M⁺- v_a^+ complexes) leading to a substantial decrease in the radiation stability of the material. Consequently, the next logical step is the investigation of isovalent cationic impurities with ionic radii larger than that of Ca²⁺ in CaF₂. An investigation of this type is already being carried out in our laboratory.

Acknowledgments

The authors are grateful to F Savihhin for the measurement of the decay kinetics, to M Kerikmäe for the CaF₂:Mn and CaF₂ samples, and to A Elango for discussion of the results. Parts of this work were supported by the Estonian Science Foundation grant No 2690 and Eurogrant INCO-COPERNICUS (contract No ERBIC15CT960721).

References

- [1] Hayes W and Stoneham A M 1985 *Defects and Defect Processes in Nonmetallic Solids* (New York: Wiley-Interscience)
- [2] Song K S and Williams R T 1993 *Self-Trapped Excitons (Springer Series in Solid State Sciences vol 105)* ed H K V Lotsch (Berlin: Springer)
- [3] Denks V, Maaros A, Nagirnyi V, Savikhina T and Vassiltsenko V 1999 *Radiat. Effects Defects Solids* at press
- [4] Sedlachek J H C and Rothschild M 1992 *Proc. SPIE* **1835** 80
Toepke I and Cope D 1992 *Proc. SPIE* **1835** 89
- [5] Eliseev E N, Zvorykin V D, Morozov N V, Sagitov S N, Sergeev P B and Fadeeva E I 1996 *Opt. Zh.* **2** 40
- [6] Schenker R, Piao F and Oldham W G 1996 *Proc. SPIE* **2726** 698
Borrelli N F, Smith Ch, Allan D C and Seward T P III 1997 *J. Opt. Soc. Am. B* **14** 1606
- [7] Leidtorp R and Petrovski G T 1980 *Dokl. Akad. Nauk SSSR* **251** 343

- Toratani H, Zou X and Matsumoto Y 1996 *Japan. J. Appl. Phys.* **35** 6351
- [8] Tomiki T and Miyata T 1969 *J. Phys. Soc. Japan* **27** 658
- [9] Heaton R A and Lin C C 1980 *Phys. Rev. B* **22** 3629
- [10] Williams R T, Kabler M N, Hayes W and Stott J P 1976 *Phys. Rev. B* **14** 725
- [11] Kalder K and Malysheva A F 1971 *Opt. Spektrosk.* **31** 252
- [12] Ershov N N, Zahharov N G and Rodnyi P A 1982 *Opt. Spektrosk.* **53** 89
- [13] Lisitsina L A, Lisitsin V M and Chinkov E P 1995 *Izv. VUZ Fiz.* **1** 13
- [14] Alonso P J and Alcalá R 1980 *J. Lumin.* **21** 147
- [15] de Melo A P, de Lima J F, Figueredo A M G, Chadwick A W and Valerio M E G 1997 *Defects in Insulating Materials* ed G E Matthews and R T Williams (Switzerland: Trans Tech) p 749
- [16] Alonso P J and Alcalá R 1981 *J. Lumin.* **22** 321
- [17] Bagai R K and Warriar A V R 1976 *Phys. Status Solidi b* **73** K123
- [18] Lushchik Ch, Liidja G, Lushchik N, Vassil'chenko E, Kalder K, Kink R and Soovi T 1973 *Luminescence of Crystals, Molecules, and Solutions* ed F Williams (New York: Plenum) p 162
- [19] Arhangelskaya V A, Lushchik N E, Reiterov V M, Soovik H A and Trofimova L M 1979 *Opt. Spektrosk.* **43** 708
- [20] Bollmann W, Görlich P, Hauk W and Mothes H 1970 *Phys. Status Solidi a* **2** 157
- [21] Arhangelskaya V A, Reiterov V M and Trofimova L M 1980 *J. Appl. Spectrosc.* **32** 103
- [22] Chorny Z P, Shchur G A, Kachan S I and Dubelt S P 1987 *Phys. Electron.* **35** 97
- [23] den Hartog H W 1996 *Radiat. Effects Defects Solids* **139** 125
- [24] Atobe K 1979 *J. Chem. Phys.* **71** 2588
- [25] Medvedeva N I, Gubanov V A, Lichtenshtein A I, Golota A F, Hodos M Ja and Kosintsev F I 1984 *J. Strukt. Khim.* **25** 147
- [26] Bianconi A, Jackson D and Monahan K 1978 *Phys. Rev. B* **17** 202